

About 2D Cavity Resonance

May 12, 2026

July 7, 2026 Revised

Takuya Yabu(takuya.yabu@live.jp)

Abstract

Research on automobile whistling and suction sounds has been conducted in the past. For cavity resonance, a type of whistling sound, the cavity resonance frequency has been determined using Rossiter's empirical equation. Therefore, we limited our study to the two-dimensional case and clarified the physical phenomena that arise by solving a set of partial differential equations that explain the phenomenon. As a result, we found that the horizontal resonance frequency becomes proportional to the speed of sound as the mainstream velocity increases, and the vertical resonance frequency decreases as the mainstream velocity increases, but when the Mach number exceeds 1, the resonance frequency no longer exists as a real number, and vertical resonance does not occur. Finally, we discussed the conditions under which resonance increases. Finally, we were able to confirm the conditions under which resonance increases through numerical calculations.

Nomenclature

L_H : Maximum hole length

ρ, c : Air density and air sound speed

ω : Angular frequency

f_x, f_y : x -direction resonance frequency and y -direction resonance frequency

k : Wavenumber

t : Time

j : Imaginary unit

U, U_{vx} : Mainstream air velocity and vortex (vorticity) velocity

κ : Ratio of vortex (vorticity) velocity to mainstream air velocity

ϕ : Empirical coefficient for phase lag

M : Mach number

ζ : Vorticity

β : Efficiency of conversion from sound pressure to vorticity

$\delta(x)$: Dirac delta function

$\delta'(x)$: Differential of Dirac delta function

$H(x)$: Heaviside step function

s : Complex number

L_y : Depth of the box

$u(x, y, t), v(x, y, t)$: Velocity in the x direction and velocity in the y direction

1. Introduction

In the past, research has been conducted on the whistling and suction sounds of automobiles (Calvo, Diaz, & San Roman, 2005) (Chien-Hsiung, Lung-Ming, Chang-Hsien, Yen-Loung, & Jik-Chang, 2009) (George, 1990) (Jagtiani, 1972) (Jung & Oh, 1995) (Münder & Carbon, 2022) (Oettle & Sims-Williams, 2017) (Qatu, Abdelhamid, Pang, & Sheng, 2009) (Wang, Chen, & Zhang, 2021) (Zhang, Meng, Li, & Zheng, 2022). Cavity resonance is a type of whistling sound. In cavity resonance, the cavity resonance frequency has traditionally been determined using Rossiter formula, an empirical formula. Therefore, for cavity resonance in the two-dimensional case, we will clarify the physical phenomena that arise by solving the set of partial differential equations that explain the phenomenon. Finally, we will examine the conditions under which resonance increases in numerical calculations.

These will be discussed below.

2. About 2D Cavity Resonance

2.1. Vorticity Movement Equation

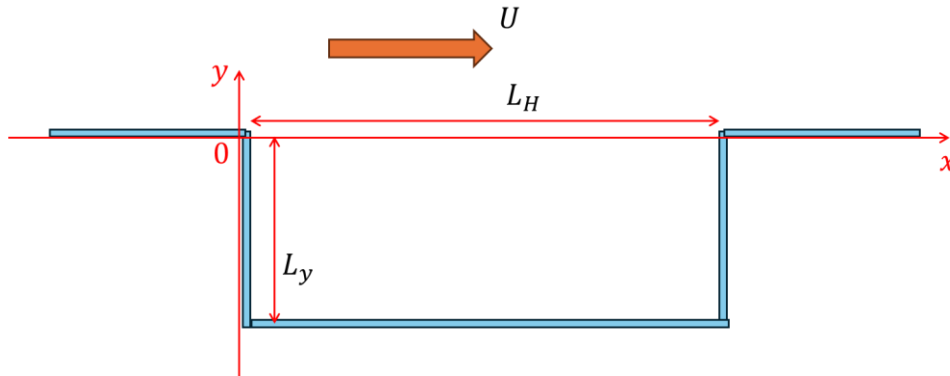


Fig. 1 2-Dimensional Box with Hole

Fig. 1 shows a box with a hole. Here, the conventional definitions of cavity resonance and cavity resonance frequency are given below.

Definition :

When air is flowing at velocity U and there is a hole, a vortex moves from

the upstream end to the downstream end of the hole. This vortex collides with the downstream end, generating sound. This generated sound then moves from the downstream end to the upstream end. Sound is a change accompanied by particle velocity, and this particle velocity then collides with the upstream end, generating another vortex. This series of phenomena is defined as "cavity resonance." Furthermore, the reciprocal of the time from when a vortex moves and generates sound until another vortex is generated is defined as the "cavity resonance frequency."

Based on this definition, we derive the differential equation representing cavity resonance, limited to two dimension. First, the movement equation of vorticity $\zeta(x, y, t)$ is expressed by the following equation. However, the viscosity term is ignored.

$$\frac{\partial \zeta}{\partial t} + U_{vx} \frac{\partial \zeta}{\partial x} = 0 \quad (1)$$

2.2. Powell's Equation

Next, we will find the relationship between sound pressure and vorticity.

Powell's equation is the relationship between sound pressure and vorticity. Expressed in two dimension, Powell's equation is given by the following:

$$\begin{aligned} & \frac{1}{c^2} \frac{\partial^2 p}{\partial t^2} - \left(\frac{\partial^2 p}{\partial x^2} + \frac{\partial^2 p}{\partial y^2} \right) \\ & = \rho [\zeta(L_H, 0, t)u(L_H, 0, t)\delta'(x - L_H)\delta(y) - \zeta(L_H, 0, t)v(L_H, 0, t)\delta(x - L_H)\delta'(y)] \end{aligned} \quad (2)$$

2.3. Initial Conditions

The initial condition for the velocity in the x -direction is given below:

$$u(x, y \geq 0, 0) = U \quad (3)$$

The initial condition for the velocity in the y -direction is given below:

$$v(x, y, 0) = 0 \quad (4)$$

The initial condition for the sound pressure is given below:

$$p(x, y, 0) = 0 \quad (5)$$

The initial condition for the time derivative of the sound pressure is given below:

$$\left. \frac{\partial p}{\partial t} \right|_{t=0} = 0 \quad (6)$$

2.4. Boundary Conditions

We need to find the boundary conditions under which the velocity of the returned particles changes to vorticity. These are given by the following equation:

$$\zeta(0,0,t) = -\beta_x \left. \frac{\partial p}{\partial x} \right|_{(x=0,y=0,t=t)} \quad (7)$$

Furthermore, assuming that sound pressure is completely reflected at the bottom of the box and becomes zero at the open end, the following conditions hold true.

$$\left. \frac{\partial p}{\partial x} \right|_{y=-L_y} = 0 \quad (8)$$

$$p|_{y=0} = 0 \quad (9)$$

Furthermore, assuming that the sound pressure is completely reflected by the left and right walls, the following conditions hold true.

$$\left. \frac{\partial p}{\partial x} \right|_{x=0, -L_y \leq y \leq 0} = 0 \quad (10)$$

$$\left. \frac{\partial p}{\partial x} \right|_{x=L_H, -L_y \leq y \leq 0} = 0 \quad (11)$$

3. Resonance Frequency of a Two-Dimensional Cavity Resonance

3.1. Solution to the Vorticity Transfer Equation

We derive the resonance frequency of a two-dimensional cavity resonance. First, we solve equation (1). The solution when the boundary condition is $\zeta(0,t)$ is given by the following equation:

$$\zeta(x,y,t) = \zeta\left(0,0,t - \frac{x}{U_{vx}}\right) \quad (12)$$

3.2. Sound Pressure Equation Using Green's Function Derived from Powell's Equation

Next, we solve Powell's equation (2). This can be obtained using the Green's function in the following form. First, the Green's function is given by the following equation.

$$G(x,y,t|L_H,0,\tau) = \sum_{n=-\infty}^{\infty} \left\{ \frac{H(c(t-\tau) - r_{n,1})}{2\pi c \sqrt{c^2(t-\tau)^2 - r_{n,1}^2}} + \frac{H(c(t-\tau) - r_{n,2})}{2\pi c \sqrt{c^2(t-\tau)^2 - r_{n,2}^2}} \right\} \quad (13)$$

Here, the following equation holds true.

$$r_{n,1} = \sqrt{(x - (2n+1)L_H)^2 + y^2} \quad (14)$$

$$r_{n,2} = \sqrt{(x - (2n+1)L_H)^2 + (y + 2L_y)^2} \quad (15)$$

From equations (2) and (13), the following equation is obtained.

$$\begin{aligned}
pp(x, y, t) = & \sum_{n=-\infty}^{\infty} \int_0^{t-\frac{r_{n,1}}{c}} \frac{\rho\beta_x \cdot \frac{\partial p}{\partial x} \Big|_{(0,0,\tau-\frac{L_H}{U_{vx}})} \cdot \Phi_{n,1}(\tau)}{2\pi c \sqrt{c^2(t-\tau)^2 - r_{n,1}^2}} d\tau \\
& + \sum_{n=-\infty}^{\infty} \int_0^{t-\frac{r_{n,2}}{c}} \frac{\rho\beta_x \cdot \frac{\partial p}{\partial x} \Big|_{(0,0,\tau-\frac{L_H}{U_{vx}})} \cdot \Phi_{n,2}(\tau)}{2\pi c \sqrt{c^2(t-\tau)^2 - r_{n,2}^2}} d\tau
\end{aligned} \tag{16}$$

Here, the following equation holds true.

$$\Phi_{n,1}(\tau) = \frac{U \cdot (x - (2n + 1)L_H) - (-1)^n \cdot v(L_H, 0, \tau) \cdot y}{c^2(t - \tau)^2 - r_{n,1}^2} \tag{17}$$

$$\Phi_{n,2}(\tau) = \frac{U \cdot (x - (2n + 1)L_H) - (-1)^n \cdot v(L_H, 0, \tau) \cdot (y + 2L_y)}{c^2(t - \tau)^2 - r_{n,2}^2} \tag{18}$$

3.3. x -Direction Resonance Frequency

Consider the resonance frequency in the x -direction. The time it takes for vorticity to propagate downstream is $\frac{L_H}{U_{vx}}$, and the time it takes for the sound to return upstream is $\frac{L_H}{c}$. Here, the phase synchronization condition is assumed to be: "Let T_x be the period of the sound produced (frequency is $f_x = \frac{1}{T_x}$). The total time taken for one cycle, $\frac{L_H}{U_{vx}} + \frac{L_H}{c}$, is equal to an integer multiple (n_x times) of the sound period, taking into account the fluid-induced generation delay (phase difference ϕ)." In this case, the following equation holds:

$$\begin{aligned}
\left(n_x - \frac{\phi}{2\pi}\right) T_x &= \frac{L_H}{U_{vx}} + \frac{L_H}{c} \\
\frac{\left(n_x - \frac{\phi}{2\pi}\right)}{f_x} &= \frac{L_H}{U_{vx}} + \frac{L_H}{c} \\
f_x &= \frac{\left(n_x - \frac{\phi}{2\pi}\right)}{\frac{L_H}{U_{vx}} + \frac{L_H}{c}}
\end{aligned} \tag{19}$$

Finally, setting $U_{vx} = \kappa U$, we obtain the following equation. This is Rossiter formula.

$$f_x = \frac{U}{L_H} \frac{\left(n_x - \frac{\phi}{2\pi}\right)}{\left(\frac{1}{\kappa} + \frac{U}{c}\right)} \tag{20}$$

3.4. y -Direction Resonance Frequency

The basic formula for the x -direction resonance frequency f_{xr} of a closed tube in stationary space is as follows:

$$f_{xr} = \frac{n_{xr} \cdot c}{2L_H} \quad (21)$$

The basic formula for the y -direction resonance frequency f_y of an open-end and closed-end tube in stationary space is as follows:

$$f_y = \frac{(2n_y - 1) \cdot c}{4L_y} \quad (22)$$

3.5. What Can Be Understood from the Resonance Frequency

By further transforming the x -direction resonance frequency in equation (20) as $U \rightarrow \infty$, the following equation is obtained:

$$f_x = \frac{U \left(n_x - \frac{\phi}{2\pi} \right)}{L_H \left(\frac{1}{\kappa} + \frac{U}{c} \right)} \rightarrow \frac{\left(n_x - \frac{\phi}{2\pi} \right)}{L_H} c \quad (23)$$

That is, the x -direction resonance frequency becomes proportional to the speed of sound as the mainstream velocity increases.

The two-dimensional resonance frequency f_{total} is given by the following equation:

$$f_{total} = \sqrt{\left(\frac{n_{xr} \cdot c}{2L_H} \right)^2 + \left(\frac{(2n_y - 1) \cdot c}{4L_y} \right)^2} \quad (24)$$

The sound pressure increases at this resonance frequency f_{total} .

3.6. Sound Pressure at a Position Outside the Sound Source ($x \geq L_H$)

We will now discuss the sound pressure at a position outside the sound source ($x \geq L_H$). As before, it can be calculated using the following equation.

$$p(x, y, t) = -\frac{\rho\beta_x}{2\pi c} \int_0^{t - \frac{\sqrt{(x-L_H)^2 + y^2}}{c}} \left[\frac{\partial^2 p}{\partial t \partial x} \Big|_{(0,0,\tau - \frac{L_H}{U_{vx}})} \Phi_{2D} - \frac{\partial p}{\partial x} \Big|_{(0,0,\tau - \frac{L_H}{U_{vx}})} \cdot \Phi_{2D} \right] d\tau \quad (25)$$

Here, the following equation holds true.

$$\Phi_{2D} = U \cdot (x - L_H) - v(L_H, 0, t) \cdot y \quad (26)$$

4. Numerical Calculations

The results were confirmed by numerical calculation. The values used are shown in

Table 1 below.

Furthermore, for $\frac{\partial p}{\partial x}$ and $v(L_H, 0, t)$, it was assumed that vortices were continuously generated at the upstream end at a Rossiter formula primary frequency of 14.4 Hz, and that this vortex mass was continuously excited at the downstream end as $v(L_H, 0, t)$ at the same Rossiter formula primary frequency of 14.4 Hz. Therefore, the following equation is continuously used during the numerical calculation. Here, $f_{x,1}$ is the Rossiter formula primary frequency of 14.4 Hz.

$$\frac{\partial p}{\partial x} = \sin(2\pi f_{x,1}t) \quad (27)$$

$$v(L_H, 0, t) = \frac{1}{2} \sin(2\pi f_{x,1}t) \quad (28)$$

Table 1 Parameter and Value

Parameter	Value
ρ	1.225(kg/m ³)
c	340.0(m/s)
U	34.0(m/s)
κ	0.6
β_x	0.01
ϕ	$\frac{\pi}{2}$
L_H	1.5(m)
L_y	0.7(m)

The numerical calculation results are shown in Fig. 2. The observation position was $(x, y) = (0.01, 0.01)$ near the origin. The top graph shows the time-series waveform of sound pressure, and the bottom graph shows the frequency characteristics of sound pressure.

Looking at the time-series waveform of sound pressure in Fig. 2, we can see that waveforms from various sound sources are combined and gradually increase in size as self-excited oscillations. In other words, it is clear that cavity resonance is self-excited.

Next, examining the frequency characteristics of the sound pressure shown in Fig. 2, a peak corresponding to the first-order frequency of Rossiter's formula f_x appears at 9.6 (Hz). A peak is also observed at 113.3 (Hz)—the first-order frequency of f_{xr} —indicating

the presence of a resonance frequency in the x -direction. Furthermore, the ratio $\frac{f_{xr}}{f_x}$ is 11.8, revealing that f_{xr} is approximately 12 times the value of f_x . This suggests that, due to the strong nonlinear distortion caused by the square-root denominator in the Green's function, when energy at 113.3 (Hz) ($n_{xr} = 1$) is redistributed into harmonics, only those harmonics that are multiples of 12 (e.g., 12x, 24x) are "pulled" into the spatial resonance cavity and appear with selectively high intensity. Conversely, regarding f_y , no oscillation is excited, even though the frequency is close to the resonance frequency of f_x .

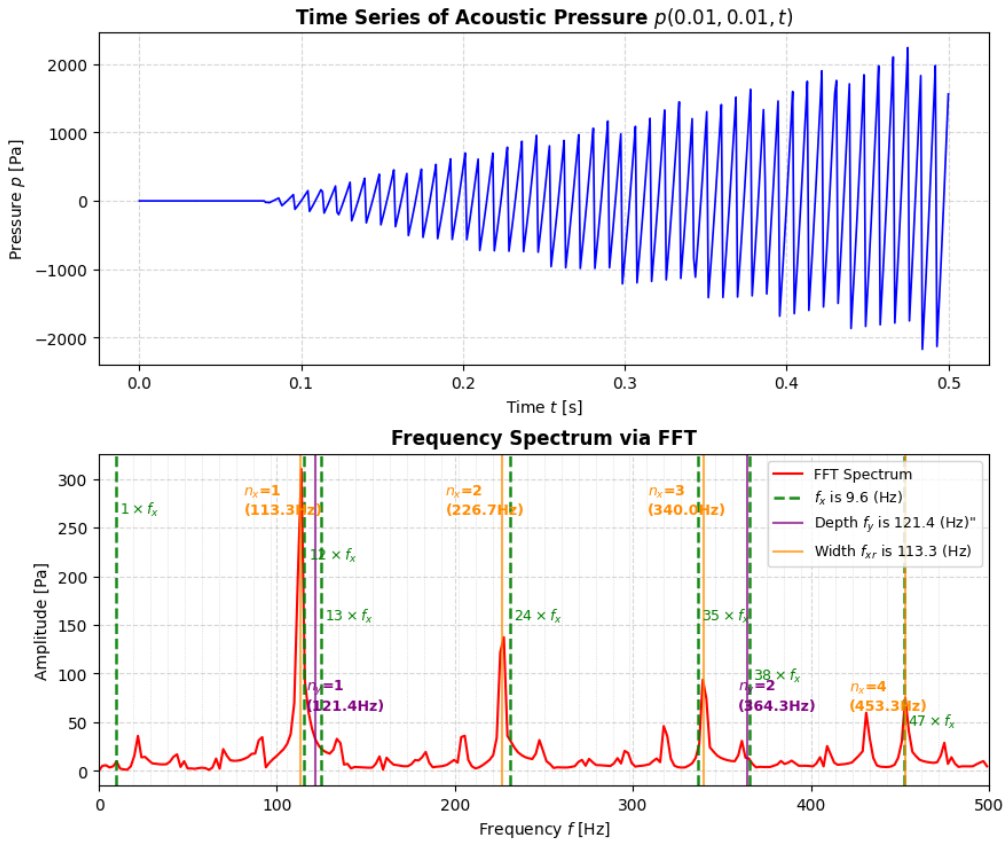


Fig. 2 Numerical Calculation Results

Next, we calculate the sound pressure for $x \geq L_H$. The results are shown in Fig. 3. The observation position was $(x, y) = (2.0, 0.5)$. The top graph shows the time-series waveform of the sound pressure, and the bottom graph shows the frequency response of the sound pressure.

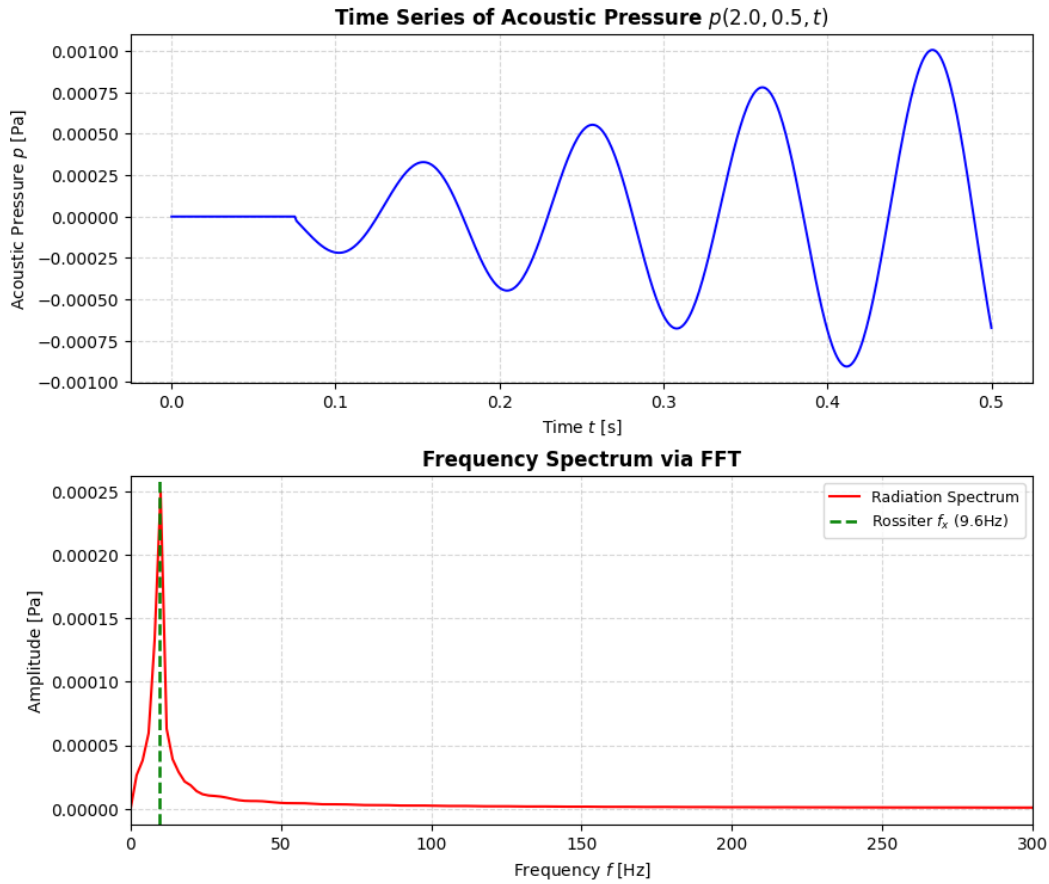


Fig. 3 Numerical Calculation Result ($(x, y) = (2.0, 0.5)$)

Looking at the top graph in Fig. 3, we can see that time is required for the sound to travel from the sound source. Also, from the frequency response below, a peak at 9.6 (Hz) appears, corresponding to the first frequency of Rossiter formula f_x . That is, for $x \geq L_H$, the sound has frequency components consisting only of the first frequency of Rossiter formula f_x , which is the frequency of forced oscillation.

Next, Fig. 4 shows the numerical calculation results for $U = 1133.3$ (m/s), with the observation point set at $(x, y) = (0.01, 0.01)$ near the origin. It can be seen that the first-order resonance frequencies of f_x and f_{xr} coincide, resulting in the generation of a very loud sound. In other words, a lock-in phenomenon is occurring.

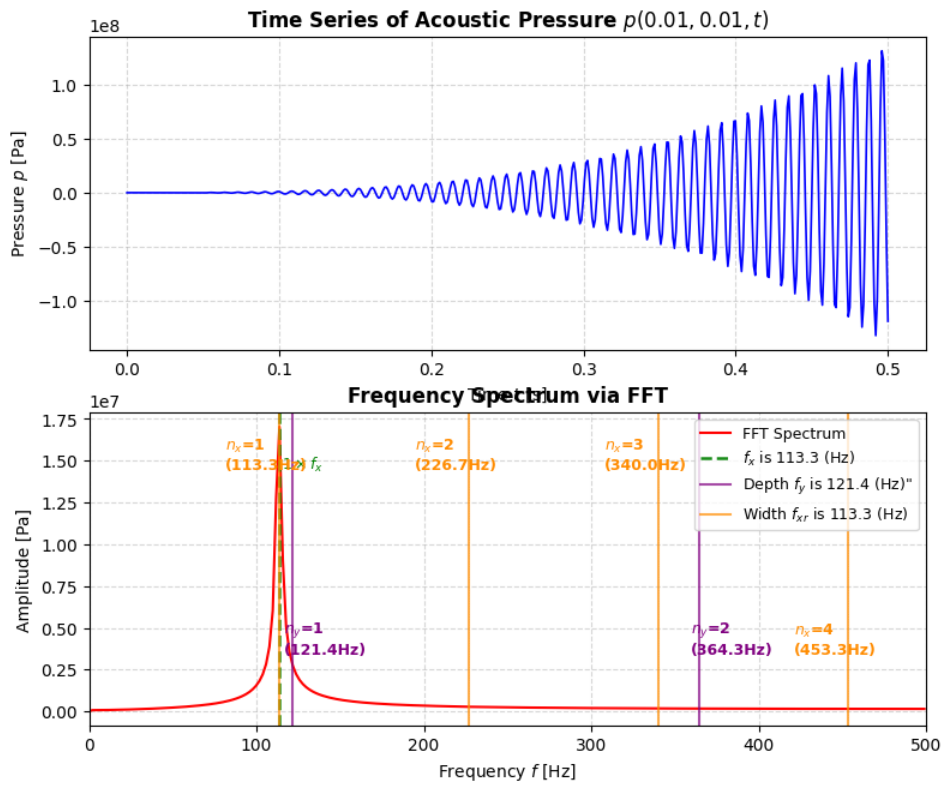


Fig. 4 Numerical Calculation Result ($U = 1133.3(\text{m/s})$)

Next, Fig. 5 shows the numerical calculation results for $U = 1700.0$ (m/s), with the observation point set at $(x, y) = (0.01, 0.01)$ near the origin. It can be seen that only the first-order resonance frequencies of f_x and f_{xr} are present.

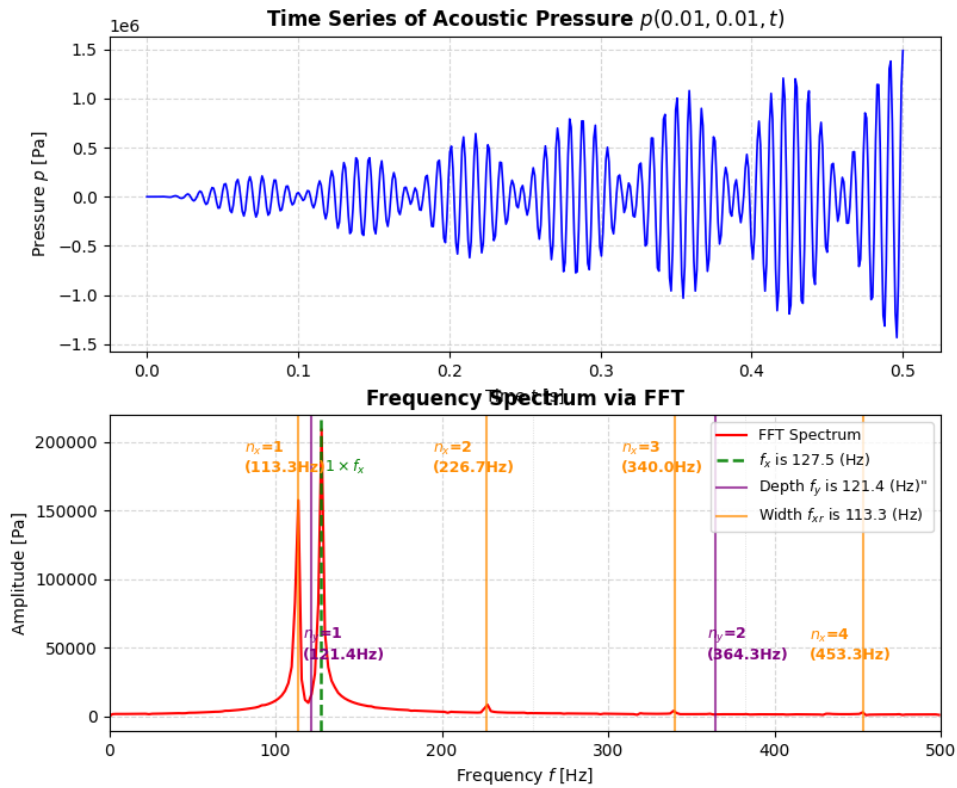


Fig. 5 Numerical Calculation Result ($U = 1700.0$ (m/s))

Finally, Fig. 6 shows the numerical calculation results for $U = 1415.5$ (m/s), with the observation point set at $(x, y) = (0.01, 0.01)$ near the origin. The first-order resonance frequency of f_x is present at the same magnitude as the first-order resonance frequency of f_y , and a peak appears at that frequency. However, no peak appears at the second-order resonance frequency of f_y . Therefore, it is considered that the resonance sound of f_x is being produced, rather than the resonance in the y-direction being excited.

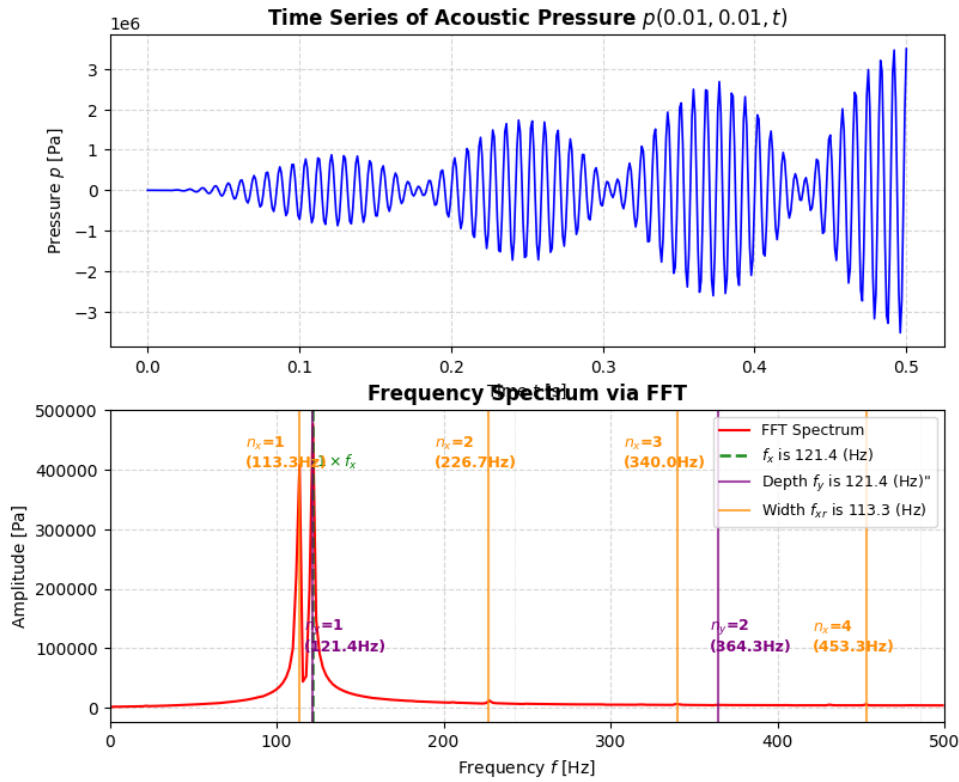


Fig. 6 Numerical Calculation Result ($U = 1415.5(\text{m/s})$)

5. Conclusion

Research on automobile whistling and suction sounds has been conducted in the past. For cavity resonance, a type of whistling sound, the cavity resonance frequency has been determined using Rossiter's empirical equation. Therefore, we limited our study to the two-dimensional case and clarified the physical phenomena that arise by solving a set of partial differential equations that explain the phenomenon. As a result, we found that the horizontal resonance frequency becomes proportional to the speed of sound as the mainstream velocity increases, and the vertical resonance frequency decreases as the mainstream velocity increases, but when the Mach number exceeds 1, the resonance frequency no longer exists as a real number, and vertical resonance does not occur. Finally, we discussed the conditions under which resonance increases. Finally, we were able to confirm the conditions under which resonance increases through numerical calculations.

References

- Calvo, J. A., Diaz, V., & San Roman, J. L. (2005). *Controlling the turbocharger whistling noise in diesel engines*. International Journal of Vehicle Noise and Vibration, Vol. 2, No. 1. doi:<https://doi.org/10.1504/IJVNV.2006.008524>
- Chien-Hsiung, T., Lung-Ming, F., Chang-Hsien, T., Yen-Loung, H., & Jik-Chang, L. (2009). *Computational aero-acoustic analysis of a passenger car with a rear spoiler*. Applied Mathematical Modelling, Volume 33, Issue 9. doi:<https://doi.org/10.1016/j.apm.2008.12.004>
- George, A. R. (1990). *Automobile Aerodynamic Noise*. SAE Transactions, Vol. 99, Section 6. Retrieved from <http://www.jstor.org/stable/44553993>
- Jagtiani, H. (1972). *The Objective Method of Evaluating Aspiration Wind Noise*. SAE Technical Paper 720506. doi:<https://doi.org/10.4271/720506>
- Jung, W., & Oh, S. (1995). *The Influence of Vehicle Elements to Aspiration Wind Noise*. SAE Technical Paper 950624. doi:<https://doi.org/10.4271/950624>
- Münder, M., & Carbon, C.-C. (2022). *Howl, whirr, and whistle: The perception of electric powertrain noise and its importance for perceived quality in electrified vehicles*. Applied Acoustics, Volume 185. doi:<https://doi.org/10.1016/j.apacoust.2021.108412>
- Oettle, N., & Sims-Williams, D. (2017). *Automotive aeroacoustics: An overview*. Journal of Automobile Engineering, Volume 231, Issue 9. doi:<https://doi.org/10.1177/0954407017695147>
- Qatu, M. S., Abdelhamid, M. K., Pang, J., & Sheng, G. (2009). *Overview of automotive noise and vibration*. International Journal of Vehicle Noise and Vibration, Vol. 5, No. 1-2. doi:<https://doi.org/10.1504/IJVNV.2009.029187>
- Wang, Q., Chen, X., & Zhang, Y. (2021). *An Overview of Automotive Wind Noise and Buffeting Active Control*. SAE International Journal of Vehicle Dynamics, Stability, and NVH, 5(4). doi:<https://doi.org/10.4271/10-05-04-0030>
- Zhang, F., Meng, W., Li, X., & Zheng, C. (2022). *A vehicle whistle database for evaluation of outdoor acoustic source localization and tracking using an intermediate-sized microphone array*. Applied Acoustics, Volume 201. doi:<https://doi.org/10.1016/j.apacoust.2022.109113>